

NANOPARTICLES FOR CANCER TREATMENT: THE ROLE OF HEAT TRANSFER

C. Thomas Avedisian¹, Richard E. Cavicchi², Paul L. McEuen³ and Xinjian Zhou³

¹Sibley School of Mechanical and Aerospace Engineering, Cornell University, Ithaca, N.Y. 14853, USA

²Department of Physics, Cornell University, Ithaca, N.Y. 14853, USA

³Process Sensing Group, National Institute of Standards and Technology, Gaithersburg, Md. 20899

ABSTRACT

An overview is presented of the role of heat transfer for cancer treatment that uses nanoparticles to deliver thermal energy to diseased areas. Nanoparticles in this process serve two functions: as carriers for therapeutic molecules on the surface of particles or encapsulated within them; and/or as materials which absorb energy when exposed to laser light of the appropriate wavelength. The role of heat transfer is central to deriving a therapeutic effect: direct delivery of heat to denature diseased cells; or stimulate release of molecular cargoes. The thermal stimulus of interest here is irradiation by a laser.

This paper presents a simple model showing parameter ranges that affect temperatures which can be achieved by laser heating of individual particles and suspensions. The results show that tight focusing is required to heat individual nanoparticles to temperatures where a therapeutic effect may be realized. A discussion of suitable metrology to measure temperature on the scale of individual nanoparticles is given based on using a single walled carbon nanotube (SWNT) as both a temperature sensor and energy absorber. SWNTs do not always Ohm's law, they may exhibit metallic or semiconductor behavior with an often unpredictable result in manufacturing, and no two SWNTs behave identically which necessitates calibration for each SWNT. Some results are presented which show the electrical characteristics of SWNTs and their potential for exploitation as a nanothermometer.

NOMENCLATURE

A	surface area
Bi	Biot number
D	beam diameter (m)
f	focal length
f_N	particle concentration in cluster
h	heat transfer coefficient
k	thermal conductivity
L	cylinder length
Nu	Nusselt number
P_L	laser power
P_L''	laser flux at particle surface
Q_1	energy absorbed by particle
r_o	beam spot size
r	radius
T_p	particle temperature
V	volume
α	fluid thermal diffusivity
ϕ	particle volume fraction
λ	laser wavelength
σ	absorption cross section
ρ	density

Subscripts

I	individual particle
f	fluid surrounding the particle or suspension
T	particle suspension

1. INTRODUCTION

Cancer is the second leading cause of death among humans. Treatment involves a combination of surgery, radiotherapy, and chemotherapy. Most of these therapies target spatial regions that are larger than the diseased area. The early work of Anderson and Parrish [1983] showed the potential for spatial confinement of heat absorbed within a biological system that could irreversibly damage cells while not harming surrounding healthy tissue. The concept was to focus a pulse laser onto a region of tissue with a greater optical absorption at the wavelength of the laser than the surrounding tissue. The development of light absorbing nanoparticles¹ which are non-toxic to biological tissue has offered the potential for a far more localized delivery of energy. When laser light of the appropriate wavelength interacts with certain types of nanoparticles, the light can trigger a photothermal effect in the particles whereby electronic oscillations at the particle surface are converted to heat which raises the particle temperature as determined by the particle's plasmon resonance. The resulting therapeutic effect is like a hyperthermia treatment but at the nanoscale.

When the particle gets comparatively hot, several effects are possible such as denaturation of cells, alterations of the permeability of the particles if functionalized with drugs that are then released to the surrounding tissue, and triggering bubble nucleation on the surface of the particle such that the growth of the bubbles imparts a mechanical stress to diseased cells that can damage them [Brinkman et al. 2000; Khlebtsov et al. 2006; Zharov et al. 2005a, 2005b, 2006; Lin et al. 1999; Hirsch et al. 2003; Kam et al. 2005; Huttman and Birngruber 1999; Kotaidis and Plech 2005]. A variety of nanoparticles have been considered for thermal therapeutics including nanospheres with metal coatings [Hirsch et al. 2003], pigmented particles [Lin et al. 1999], gold nanoclusters and particles [Zharov et al. 2005a; Kotaidis and Plech 2005], and gold nanorods. In some variations of thermal therapeutics, the laser also serves as a catalyst to release materials encapsulated in the nanoparticles by increasing the permeability of the particle wall upon being heated [Skirtach et al. 2005].

The efficacy of photothermal treatment depends on the ability of the energy absorbers to locally heat diseased areas without damaging healthy tissue. An "optical window" (referred to by Anderson and Parrish [1983]) must exist whereby the particles are strongly absorbing at the wavelength of the laser while the surrounding (healthy) tissue is transparent. In this event, only the particles are heated and the background absorption effects would be negligible. Such is the case for certain types of nanoparticles in the near infrared (NIR) where the nanoparticles are strongly absorbing while tissue (e.g., most animal cells and tissues [West and Halas 2000; Konig 2000; Weissleder 2001; Kam et al. 2005; Cherukuri et al. 2004; O'Neal et al. 2004]) are relatively transparent. Several types of nanoparticles have been

considered for this purpose², such as unconjugated gold nanoshells, nanorods and nanosheets, and single walled carbon nanotubes (SWNT)[Hirsch et al. 2003, Kam et al. 2005, O'Neal et al. 2004, Panchapakesan et al. 2005, Zharov et al. 2005a 2005b 2006] the latter of which are cylinders of nanometer diameter consisting of a single sheet of graphene wrapped up to form a tube [McEuen et al. 2002]. The nanoparticles themselves must be non-toxic to be effective and many of those which have been developed for this purpose satisfy this requirement.

Temperature is the most important variable to control as the damage threshold for killing cells and the thermodynamic state of tissue required to trigger a phase change (which under some conditions can be explosive leading to the concept of a 'nanobomb' [Panchapakesan et al. 2005, Zharov et al. 2005a]) is determined almost entirely by temperature. Recent studies on nanoparticle/laser interactions in suspension have shown definite thermal effects of the laser on the average fluid state [Hirsch et al. 2003; Kam et al. 2005]. However, there is some question on the extent to which these effects can be localized to the surface of the particle [Kebblinski et al. 2006]. The evidence of phase change noted above suggests that there must be significant superheating localized to the scale of the particle under some conditions and that it must occur. At the same time, the ability to achieve this result depends on the magnitude and duration of the laser pulse.

The present study addresses the heating process initiated by interaction of a particle with a laser. A simplified continuum model (valid because the mean free path in liquids and amorphous solids is on the order of atomic distances [Kebblinski et al. 2006]) is used to identify parameters that can produce significant temperature changes localized to the nanoparticle. Since the ability to measure the effect of laser interaction on individual nanoparticles requires sensing temperature on the nanoscale, the last section presents an approach to do this based on developing an SWNT as a temperature sensor.

2. MODELING LASER HEATING OF NANOPARTICLES

The physical situation is schematically shown in figure 1. A nanoparticle suspension is exposed to a laser at some focal distance f from the lens. The laser penetrates the fluid and is partly absorbed by the nanoparticles. The energy absorbed by the particles is then transferred to their immediate surroundings.

¹The term "nanoparticle" includes single walled nanotubes (SWNT), double walled nanotubes, nano-spheres, nano-rods, nano-shells, or nano-sheets.

²O'Neal et al. [2004] and Oldenburg et al. [1998] demonstrated a tunability for certain types of nanoparticles (e.g., silica cores with an ultrathin metallic gold coating) that arises by varying the thickness of the coating.

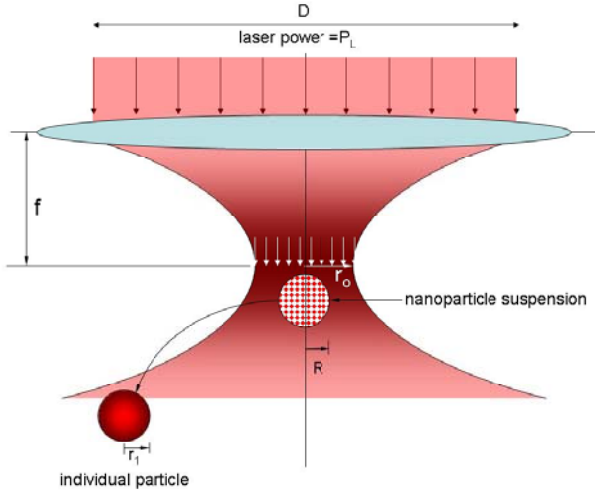


Figure 1: Schematic of laser/particle interaction where the nanoparticles are confined to a region R. r_o is the focused beam spot size, f the focal length, P_L the laser power and D the incident beam diameter (not to scale).

For the temperature rise of the particle to be significant, the thermal wave which emanates from the particle as a result of it being heated should be confined to a small distance from the particle surface. Figure 2 illustrates the situation. Taking as a characteristic length the particle radius, $r_1 < 100\text{nm}$, and assuming that $\alpha \sim 1.6 \times 10^{-7} \text{ m}^2/\text{s}$ (e.g., water) as representative, laser pulse durations $\tau \sim r_o^2/\alpha$ less than 60ns

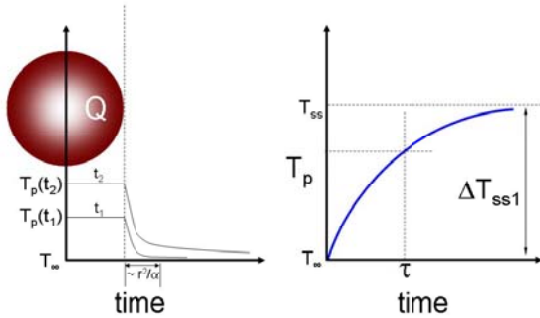


Figure 2: Schematic of the temperature distribution around a particle.

would be required to achieve high localized temperatures. Pulse lasers are thus suitable for thermal confinement of absorbed energy. In fact, computed particle temperatures from pulse heating can be on the order of several thousand degrees [Pitsillides et al. 2003; Khlebtsov et al. 2006] which would certainly lead to particle destruction if not explosive boiling of fluid. Bubble nucleation triggered by pulse heating nanoparticles has been experimentally demonstrated (e.g., Zharov et al. [2005a 2005b]).

For sufficiently long exposure times the laser energy will be dissipated to the surrounding and a steady state will be reached. This is the situation for continuous wave laser heating. A simple steady state model shows the relationship

among parameters that could yield particle temperatures of some therapeutic benefit even under continuous wave heating. And recent experiments on particle suspensions of SWNTs do show substantial heating from a continuous wave laser [Kam et al. 2005].

An estimate of the steady state particle temperature balances the energy absorbed by the particle with the energy lost to the surroundings. Temperature gradients in the particle will be negligible since the Biot number, $Bi = hr_1/k_1 \ll 1$. Assuming that heat transfer between the particle and surrounding is measured by the Nusselt number, $Nu = hr_1/k_f$, where h is the heat transfer coefficient, the Biot number can be expressed as $Bi = Nu \frac{k_f}{k_1}$. If a pure conduction process is

assumed between the particle and surrounding, and furthermore that the particle shape is spherical, then $Nu_{r1} \sim 1$. $k_f \sim 0.63 \text{ W/mK}$ (water) and $k_1 \sim 3000 \text{ W/mK}$ (SWNT, Kim et al. [2001]) or 318 W/mK (gold, [Lide 2000]) shows that $Bi \ll 1$. The particle temperature is then spatially uniform and temporally varying. The more general case for a spherical particle is captured by the correlation [Incropera et al. 2007] $Nu_{r1} = 1 + f(Ra, Pr)$ where

$$f(Ra, Pr) = 0.495 \frac{Ra_{r1}^{1/4}}{\left[1 + \left(\frac{0.469}{Pr}\right)^{9/16}\right]^{4/9}}, \quad Ra_{r1} \text{ is the Rayleigh}$$

number based on the particle radius and Pr is the fluid Prandtl number. Taking properties of water as typical and $r_1 \sim 65 \text{ nm}$ shows that $f(Ra, Pr) \ll 1$. This means that conduction is a reasonable mode for heat transport between such small spherical particles and the surrounding ambient fluid.

Consider first a single isolated nanoparticle. The steady state particle temperature corresponds to the laser energy absorbed by the particle, Q_1 , being balanced by heat loss to the fluid. The steady state temperature rise of the particle is expressed as

$$\Delta T_1 = \frac{Q_1 r_1}{Nu_{r1} A_1 k_f} \quad 1$$

The absorbed energy for an individual particle is related to the heat flux at the surface of the particle as

$$Q_1 = P_L \sigma \quad 2$$

where σ (m^2) is the absorption cross section³. The heat transfer coefficient can be determined if the temperature distribution surrounding the particle is known. The pure conduction

³The absorption cross section can also be reported in terms of an 'efficiency factor' of absorption, K , as $\sigma = \pi r_1^2 K$ with K found to be on the order of 0.1 to 1.0 in the NIR for gold nanospheres (Pustovalov and Babenko 2004), or in terms of the molar absorption cross section, σ' (m^2/mole of carbon) as for SWNTs (Murakami et al. 2005).

Nusselt number for a spherical particle in an infinite medium based on particle radius is $Nu_{r_i}=1$. For a nanotube of cylindrical shape, there is no solution for the steady state temperature distribution for conduction from a cylinder. Koblinski et al. (2006) modeled a cylindrical nanoparticle as a composite cylinder with a temperature at infinity extending over a distance equal to the cylinder length, L_1 to arrive at $\Delta T_1 = \frac{Q_1}{2\pi r_i k_f} \ln \frac{L_1}{r_i}$. This result is obtained from eq. 1 by

using a conduction Nusselt number for a composite cylinder which has the analytical representation $Nu_{r_i} = \frac{1}{\ln \frac{L_1}{r_i}}$. A

collection of correlations for Nusselt number for a wide range of geometries and convective flow conditions is given in Incropera et al. [2007].

For an aggregate of particles in suspension within a radius $L_T=R_T$ and volume V_T which is at a uniform temperature, the total absorbed energy in the suspension is $Q_T=NQ_1$ (i.e., particle volume fraction $\phi = V_T f_N$ where the particle concentration is f_N). Eq. 1 is modified as

$$\Delta T_s = \frac{(NQ_1)R_T}{Nu_{L_T} A_T k_f} \quad 3$$

where $N = \phi \frac{V_T}{V_1}$. In terms of the volume fraction, ϕ , eq. 3 can be written as

$$\Delta T_s = \phi \frac{Q_1 R_T}{Nu_{r_i} A_i k_f} \quad 4$$

which gives the ratio of suspension to local temperature rise from eqs. 1 and 4 as $\frac{\Delta T_s}{\Delta T_1} = \phi \frac{R_T}{r_i}$. The characteristic length scale of a suspension of particles may also be taken as the beam spot size which illuminates the suspension.

For the gold nanoparticles fabricated by Hirsch et al. (2003), and using the reported parameters of $\sigma=3.8 \times 10^{-14} \text{ m}^2$, $P_L=4 \times 10^4 \text{ W/m}^2$, $f_N=4.4 \times 10^{15} \text{ m}^{-3}$, $r_i=75 \text{ nm}$, and $Nu_{r_i}=1$, Eq. 1 predicts that $\Delta T_1=0.0027\text{K}$. Thus, at the scale of the nanoparticle itself the temperature change should be insignificant when the suspension is heated by a continuous wave laser. However, measured temperatures obtained from magnetic resonance temperature imaging (MRTI) show an increase of ten or more degrees above the surrounding tissue, which was sufficient to cause cell damage. Figure 3 from Hirsch et al. [2003] shows the effect of exposure of the nanosphere suspension to a continuous wave NIR laser ($\lambda=820\text{nm}$) which illustrates the destructive effect which absorption of the laser energy has on the tissue.

From the above estimate, it does not appear possible that steady state conditions localized to individual particles are capable of raising the particle temperature to the value required for damaging cells. At the same time, we know that cell damage did occur based on the work of Hirsch et al. [2003] who reported the effects of exposure of mouse tissue with nanoparticles to an NIR laser. Figure 3 shows such damage as a result of particle heating.

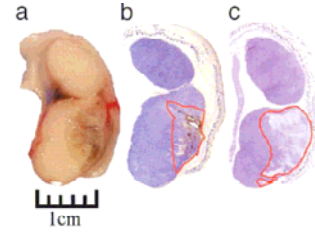


Figure 3: MRTI images of mice tissue showing irreversible damage (Hirsch et al. 2003): a) overall view of tissue; b) region of localized nanoshells in red; c) area showing tissue damage after exposure.

Considering, however, a particle suspension and using a beam spot size (R_T) of 5mm as reported by Hirsch et al. [2003] in eq. 3 leads to a prediction of $\Delta T_s=93\text{K}$ which is the right order of magnitude relative to the measurements. Reducing R_T to 4mm brings the temperature rise into closer agreement with the measured values.

The experiments of Kam et al. (2005) showed the ability of SWNT suspensions to deliver enough energy to diseased tissue to raise the average temperature of the liquid when exposed to a $1.4 \times 10^4 \text{ W/m}^2$ laser at $\lambda=808\text{nm}$ for two minutes. Temperature measurements *in vitro* of the suspension in a cuvette were made in 20s intervals with a bulk thermocouple inserted in the cuvette. The results are given in figure 4.

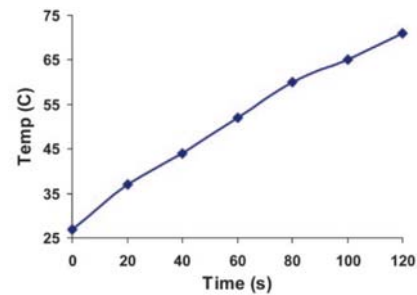


Figure 4: Variation of average temperature of a suspension of SWNTs while exposed to a 2 minute pulse of an NIR laser (Kam et al. 2005).

The increase of temperature shown in figure 4 was attributed to the SWNTs acting as "tiny NIR heaters", implying a thermal effect localized to the scale of the particle. To examine if temperature can be so localized, we again use eq. 1 to estimate the temperature rise. Assuming that the conduction Nusselt number is between 0.1 and 1 for a cylinder

(e.g., for a concentric cylinder with aspect ratio 1000, $Nu_{r_1} \sim 0.14$) and using properties of the experiment of Kam et al. (2005) - $\rho_1 \sim 1400 \text{ kg/m}^3$, $L_1 \sim 1 \mu\text{m}$, $r_1 \sim 1 \text{ nm}$ (Nikolaev et al. 1999), $\sigma' \sim 100 \text{ m}^2/\text{moleC}$ in the NIR (Murikami et al. 2005) and $P_L = 1.4 \times 10^4 \text{ W/m}^2$, and $k_f \sim 0.63 \text{ W/mK}$ (water) - eq. 1 predicts a negligible ΔT_1 .

Considering eq. 3 for a suspension of particles, Kam et al. (2005) confined a 25mg/l mixture of SWNTs in a cuvette 3 cm diameter and 1 cm high. Heat transfer from the cuvette was presumably to room temperature air by natural convection. Representative heat transfer coefficients for natural convection in gases lie between $2 \text{ W/m}^2\text{K}$ and $25 \text{ W/m}^2\text{K}$ and $k \sim 0.03 \text{ W/mK}$ (Incropera et al. 2007). For a characteristic length of the cuvette as $L_T \sim 0.015 \text{ m}$ the Nusselt number ranges between 1.0 and 10. which from eq. 3 corresponds to $8 \text{ K} < \Delta T < 100 \text{ K}$. Considering the simplicity of the estimate and the uncertainty of the input parameters, this range is remarkably close to the measurements of figure 4.

Continuous heating of nanoparticles may provide localized energy delivery if parameters are suitably adjusted. Since $P_L = P_L / (\pi r_o^2)$ and taking a long aspect ratio cylindrical particle (e.g., SWNT) of length L_1 and radius r_1 eq. 1 becomes

$$r_o = \left(\frac{P_L \sigma}{2\pi^2 Nu_{r_1} k L_1 \Delta T} \right)^{1/2}. \quad \text{With information on the optical}$$

cross section of SWNT given in terms of a molar absorption coefficient (Murakami et al. 2005), σ' (m^2/mole of carbon),

$$\sigma = \sigma' \frac{\rho (4\pi r_1^2 L_1)}{W}, \text{ then}$$

$$r_o = \left(\frac{2 P_L \sigma' r_1^2 \rho}{\pi Nu_{r_1} k W \Delta T} \right)^{1/2} \quad 5$$

We selected the following conditions: $Nu \sim 0.10$ as representative of conduction for lengths scales typical of SWNTs; particle radii between 1nm and 5nm which encompass a range typically found in various SWNT manufacturing processes; a laser power of 10W as an upper value of commercial continuous wave lasers; thermal conductivity of $k_f \sim 0.6 \text{ W/mK}$ (representative of a bio system with properties of water); and molar absorption cross section $\sigma' = 100 \text{ m}^2/\text{moleC}$ for an SWNT (Murakami et al. 2005).

Fig. 5 shows the influence of temperature rise and particle radius on the required focusing size for a 10W cw laser.

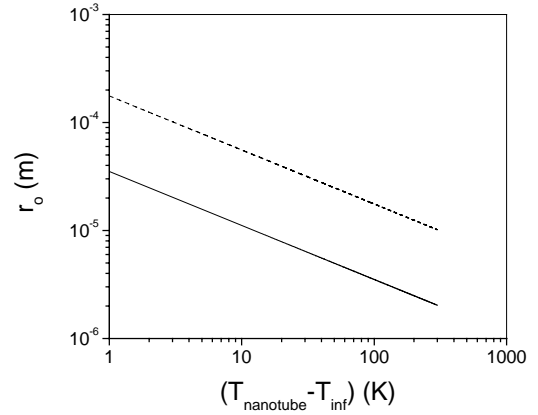


Figure 5: Computed laser spot size for different temperature increases in water for a 1nm and 5nm diameter SWNT. Dotted line, 5nm radius SWNT; solid line, 1nm radius SWNT.

The calculations are taken up to $\Delta T = 300 \text{ K}$ which is the superheat limit of water (Avedisian 1985) to cover temperatures that would induce bubble nucleation, a process that was examined for pulse laser heating of nanoparticles by Zharov and co-workers (Lapotko et al. 2002; Zharov et al. 2005a, 2005b). For a 10K rise in temperature - a value that would have a therapeutic effect - a focal spot size between $10 \mu\text{m}$ and $60 \mu\text{m}$ is required. For $\Delta T = 300 \text{ K}$ the required spot size for a 5 nm particle is about $10 \mu\text{m}$.

The predicted spot sizes in figure 5 do not conflict with the diffraction limited focal length, $f > \frac{2}{1.22} \frac{r_o D}{\lambda}$ for

reasonable values of the parameters. For example, $\lambda = 808 \text{ nm}$, $D = 1 \text{ mm}$, $r_o = 10 \mu\text{m}$ and $\Delta T = 10 \text{ K}$ yields a diffraction limited focal length of about 20mm. A longer focal length allows for greater depth probing of tumors.

The only reported study of laser heating of SWNTs was for an SWNT suspension (Kam et al. 2005) under conditions where the particles themselves could not be heated to appreciable temperatures as discussed previously. The limitations were principally the low laser power and large focal area of the experiments. The calculations in figure 5 show that tight focusing is required to achieve high temperatures localized to the nanoparticle.

The previous estimates show that significant heating of spherical nanoparticles can be achieved by adjusting laser parameters. Some recent work has also reported measuring temperature on the scale of an individual nanosphere in a suspension [Hartland 2004]. We next discuss the potential for a direct way to measure temperature of an SWNT.

3. NANOTHERMOMETRY WITH A NANOTUBE

A direct way to measure temperature localized to the scale of an SWNT is to use the SWNT as both the energy absorber and thermometer, much like a thermistor. Other approaches such as MRTI [Hirsch et al. 2003] or fluorescence

imaging of micrometer-sized capsules [Skirtach et al. 2005] provide a more spatially averaged thermal profile around clusters. Considering the different geometries of nanoparticles that have been developed - spheres, shells rods and cylinders - the SWNT may also be the most convenient one for development as a thermistor because of its cylindrical shape.

SWNTs have a number of advantages for serving as a nano-temperature sensor. The optical window of SWNTs in the NIR has already been noted. SWNTs by themselves are not toxic when functionalized with certain anti-cancer therapies (e.g., certain proteins [Kam et al. 2004]). The electrical resistivity of an individual SWNT can have a strong dependence on temperature, at least at room temperature and lower which is where virtually all of the data have been reported (e.g., Fischer et al. 1997; Kane et al. 1998). The trends at low temperature cannot be extrapolated to temperatures above room temperature. The technology for fabricating electronic packages of single SWNTs bridging metal electrodes [Cao et al. 2004 2005; Heller et al. 2005; Franklin et al. 2002] makes it viable to envision a single SWNT as a monitor for temperature sensing during laser heating. We discuss here some recent efforts to develop an SWNT into such a capability.

SWNTs pose unique challenges for temperature sensing. They tend to be non-ohmic in the sense that current is not linear with voltage. They are fragile and subject to failure on exposure to static charge. SWNTs can behave like transistors and shut off current above a threshold bias voltage. No two SWNTs are alike so that a universal resistivity calibration will not exist for SWNTs and each SWNT is unique and its electrical characteristics must be measured for the application. Some SWNTs are metallic with a resistance that increases with temperature while others behave like a semiconductor and it is not possible to predict which type of SWNT will result from a given fabrication process. And during calibration the SWNT must be exposed to temperatures significantly above room temperature. The behavior of individual SWNTs behavior at such temperatures is largely unexplored.

Some of the above challenges have been addressed in prior work. Electronic packages incorporating single isolated SWNTs have been fabricated in connection with a variety of applications unrelated to the present one, including using SWNTs as nanoelectrodes for electrochemistry studies using carbon nanotubes as field-effect transistors and in connection with fundamental studies of electrical transport in SWNTs [Mann et al. 2003, Cao et al. 2004 2005, Heller et al. 2005, Javey et al. 2003, McEuen et al. 2002]. The configurations have included SWNTs freely suspended, or lying on a substrate. In the following we present some results which suggest the potential for SWNTs for measuring temperature significantly above room temperature.

In the fabrication process the point of attachment of SWNTs to metal electrodes could produce a contact resistance, R_c , that would have to be considered in the analysis of the electrical signal. The concern with contact resistance was

recently addressed [Pop et al. 2005; Mann et al. 2006; Cao et al. 2005] in which it was pointed out that platinum and gold electrodes provide a comparatively low contact resistance relative to the resistance between the electrodes. Typically, R_c is an order of magnitude less than R_{cnt} [Pop et al. 2005; Arai et al. 2004; Franklin et al. 2002]. To estimate the contact resistance, a model to predict current flow in an SWNT should be used with the contact resistance as a fitting parameter for the voltage.

The small size of SWNTs, order of several nm diameter and a few micrometers long, motivated an integrated fabrication process in which the SWNT is grown across the electrodes. The process is described by McEuen et al. [2002], Sazonova [2006] and Cao et al. [2005]. The fabrication process begins with an Si wafer that is degeneratively doped with a 500nm layer of SiO_2 . A 50nm metal layer of Au is then evaporated on top of the SiO_2 . $\text{FeO}_3/\text{MoO}_2$ catalyst pads are photolithographically patterned on the Au. The assembly is then placed in a chemical vapor deposition furnace with a constant flow of methane to grow the nanotube. The SWNTs grow from pad to pad with the aid of a wet etching step in buffered oxide. After etching, a drying step is performed to prevent the SWNT from sticking to the substrate. The end result is a SWNT that bridges across the electrodes. With this method, a package that contains one or a few nanotubes can be created. It is not possible to know how many SWNTs are grown across the metallic pads until a current is measured for a given bias voltage.

Figure 6 is a photomicrograph of the electronic packages used in the fabrication process. The metallization pattern is shown by the bright yellow lines. The lines terminate in 'tees' across which the SWNT would grow. The SWNTs grown on the chips of fig 6 ranged from 1nm to 5nm and were around 10-12 μm long.

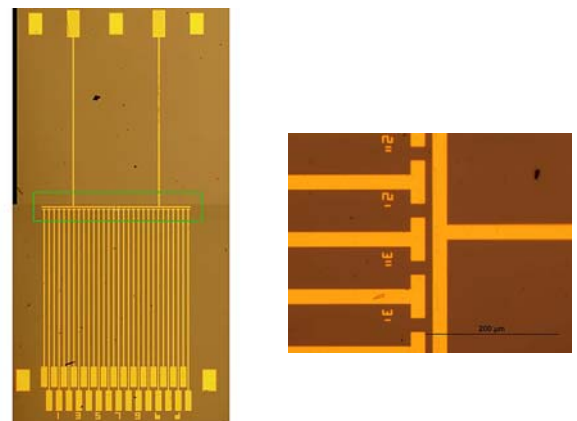


Figure 6: Photomicrograph of a nanotube package. Numbered pads at bottom and two pads at top are contacts for measuring the bias voltage. The other pads (without lines) are gate voltage pads. Nanotubes (not visible) are grown across the gap within the zone marked by the green rectangle. Visible metallization is gold and the substrate is Si. Some of the packages had a Cr underlayer for enhanced adhesion.

Some of the packages also included a 50nm sublayer of Cr to provide enhanced adhesion of the gold. Without the Cr layer, the pads for electrical contact were quite fragile and often tended to scratch on the probe station during measurements.

After fabrication, the package is annealed in an oven at 400C to 600C by an 'ashing' procedure to improve the contact resistance and clean the surface of residues associated with processing. Electrical connections to the pads shown in figure 6 were made by probe station contacts in which the measurements were made. A hot plate is integrated with the probe station to allow determination of the influence of temperature. The procedure was to slowly vary the temperature of the hot plate from room temperature to about 300C - the highest temperature at which we are aware for measuring the electrical characteristics of SWNTs. The current through the SWNT was measured by scanning voltage from -2V to +2V at each temperature. The measurements were automated with LABView control. An example of one voltage scan in air is shown in figure 7.

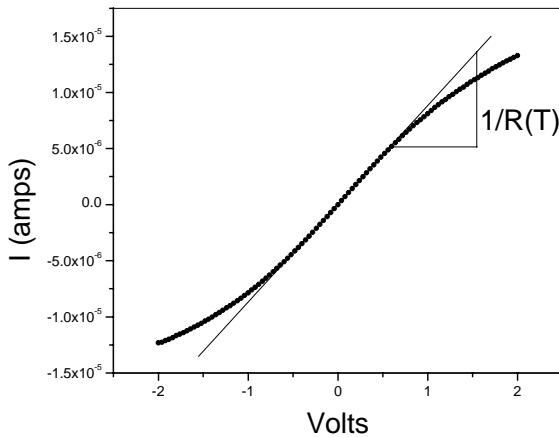


Figure 7: Variation of current with voltage of a SWNT. Linear portion around $V = \pm 0.5V$ determines the resistance.

For a given SWNT the measurements were repeatable, though it was also found that two different SWNTs behaved differently. Electrical characteristics of suspended SWNTs were previously reported up to around 125C [Pop et al 2006]. We extended this range for substrate supported SWNTs to about 300C. The relationship between current and voltage was found to be linear only around the origin ($\pm 0.5V$) and it is in this range that the resistance was determined. Distinct nonlinearities existed at higher bias voltages. This trend indicates non-Ohmic behavior of the SWNT. It may be due to nonisothermal conditions existing at high voltage biases because of self-heating or to scattering of optical phonons at high bias [Pop et al. 2005].

A plot of the resistance (inverse slope of the linearized data in figure 7) with temperature is shown in figure 8.

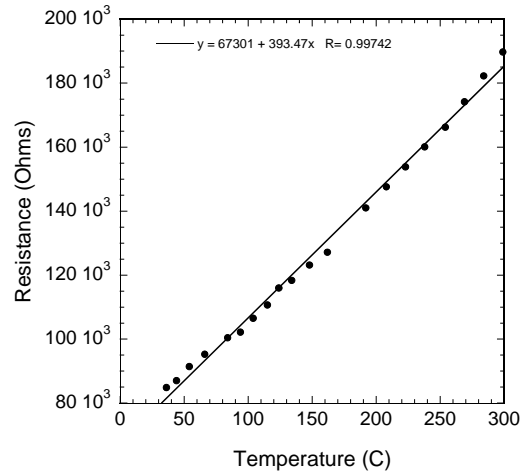


Figure 8: Variation of resistance with temperature for an SWNT.

Over the temperature range indicated, the variation is reasonably linear for this particular SWNT with nominal values in the range of several hundred k Ω . As previously noted, the quantitative measurements shown in figure 8 would not apply to a different SWNT. This fact was typical of all the SWNTs we have thus far characterized.

6. CONCLUSIONS

The ability of continuous laser heating to significantly increase the temperature of individual nanoparticles in suspension is possible only by tightly focusing the laser. A direct measurement of the local temperature that results from optical heating is the best way to verify the relationship among parameters but this is challenging in its own right. Fashioning an SWNT into a sensor may offer such a capability. It is shown that SWNTs have a strong dependence of electrical resistance with temperature up to 300C which suggests their use as a thermistor. At the same time, the electrical characteristics are unique to each SWNT and would have to be measured individually. The non-Ohmic behavior of SWNTs at high voltages restricts the range over which measurements of voltage and current can be used to determine electrical resistance as a function of temperature.

ACKNOWLEDGMENTS

This project was supported by the New York State Office of Science, Technology and Academic Research. The laboratory assistance of Mr. Johannes Kutten and conversations with Dr. Joseph T. Hodges are greatly appreciated.

REFERENCES

- Anderson, R.R. and Parrish, J.A. 1983 *Science*, 220, 525-527.
- Arai, F., Ng., C., Liu, P., Dong, L., Imaizumi, Y., Maeda, K. Proc. 2004 4th IEEE Conference on Nanotechnology, 146-148.
- Avedisian, C.T., 1985 *J. Phys. Chem. Ref. Data*, 14(3), 695-720.
- Brinkmann, R., Huttmann, G., Rogener, J., Roeder, J., Bimgruber, R. and Lin, C.P. 2000 *Lasers Surg. Med.* 27, 451-464.
- Cao, J., Wang, Q., Wang, D. and Dai, H. *Small* 2005 1, 138-141.
- Cao, J., Wang, Q., Rolandi, M. and Dai, H. 2004 *Phys. Rev. Lett.* 93, 216803.
- Cherukuri, P., Bachilo, S.M., Litovsky, S.H., and Weisman, R.B. 2004 *J. Am. Chem. Soc.*, 126, 15638-15639.
- Fischer, J.E., Dai, H., Thess, A., Lee, R., Hanjani, N.M., Dehaas, D.L. and Smalley, R.E. 1997 *Phys. Rev. B.* 55, R4921-R4924.
- Franklin, N.R., Wang, Q., Tomblor, T.W., Javey, A. and Shim, M. 2002 *Appl. Phys. Lett.* 81, 913-915.
- Hartland, G.V. 2004 *Phys. Chem. Chem. Phys.* 4, 5263-5274.
- Heller, I., Kong, J., Heering, H.A., Williams, K.A., Lemay, S.G. and Dekker, C. 2005 5, 137-142.
- Hirsch, L.R., Stafford, R.J., Bankson, J.A., Serhsen, S.R., Rivera, B., Price, R.E., Hazle, J.D., Halas, N.J., West, J.L. 2003 *Proc. Nat. Acad. Sci.* 100, 13549-13554.
- Huttmann, G., and Birngruber, R. 1999 *IEEE J. Selected Topics in Quantum Electronics*, 5(4) 954-962.
- Incropera, F.P., DeWitt, D.P., Bergman, T.L., Lavine, A.S. 2007 *Introduction to Heat Transfer*, 5th ed., pp. 8, 547, chapters 6-9, New York, John Wiley.
- Javey, A., Guo, J., Wang, Q., Lunnstrom, M. and Dai, J. 2003 *Nature*, 424, 654-657.
- Kam, N.W.S., Jessop, T.C., Wender, P.A. and Dai, H. 2004 *J. Am. Chem. Soc.* 126, 6850-6851.
- Kam, N.W.S., O'Connell, M., Wisdom, J.A. Dai, H. 2005 *Proc. Nat. Acad. Sci.* 102, 11600-11605.
- Kim, P., Shi, L., Majumdar, A. McEuen, P.L. 2001 *Phys. Rev. Lett.* 87, 215502.
- Kebllinski, P., Cahill, D.G., Bodapati, A., Sullivan, C.R., Taton, T.A. 2006 *J. Appl. Phys.* 100, 054305.
- Khlebtsov, B., Zharov, V., Melnikov, A., Tuchin, V., Khlebtsov, N. 2006 17, 5167-5179.
- Konig, K. 2000 *Journal of Microscopy*, 200, Pt 2, 83-104.
- Kotaidis, V. and Plech, A. 2005 *App. Phys. Lett.* 87, 213102.
- Lapotko, D.O., Romanovskaya, T.R. Schnip, A. and Zharov, V. 2002 *Lasers Surg. Med.* 31, 53-63.
- Lide, D.R. 2000 *Basic Laboratory and Industrial Chemicals*, p. 151, Boca Raton, CRC Press.
- Lin, C.P., Kelley, M.W., Sibayan, A.B., Latina, M.A., Anderson, R.R. 1999 *IEEE J. Quantum. Elec.* 5, 963-968.
- Mann, D., Javey, A., Kong, J., Wang, Q. and Dai, H. 2003 *Nano Lett.* 3, 1541-1544.
- Mann, D., Pop, K.E., Cao, J., Wang, Q., Goodson, K. and Dai, H. J. 2006 *Phys. Chem. B*, 110, 1502-1505.
- Murakami, Y., Einarsson, E., Edamura, T., Maruyama, S. 2005 *Phys. Rev. Lett.* 94, 087402.
- McEuen, P.L., Fuhrer, M.S. and Park, H. 2002 *IEEE Trans. Nanotech.* 1, 78-85.
- O'Neal, D.P., Hirsch, L.R., Halas, N.J., Payne, J., West, J.L. 2004 *Cancer Letters*, 209,171-176.
- Panachapakesan, B., Shaoxin, L., Sivakumar, K., Teker, K., Cesarone, G., Wickstrom, E. 2005 *NanoBiotech.*1, 133-139.
- Pitsillides, C.M., Joe, E.K., Wei, X., Anderson, R.R., Lin, C.P. 2003 *Biophys. J.* 84, 4023-4032.
- Pop, E., Mann, D., Cao, J., Wang, Q., Goodson, K., Dai, H. 2005 *Phys. Rev. Lett.* 95, 155505.
- Pop, E., Mann, D., Cao, J., Wang, Q., Goodson, K., Dai, H. 2006 *Nano Letters*, 6(1), 96-100.
- Pustovalov V.K. and Babenko, V.A. 2004 *Laser Phys. Lett.* 1, 516-520.
- Sazonova, V.A. 2006 "A tunable carbon nanotube resonator," Ph. D Thesis, Dept. of Physics, Cornell University.
- Skirtach, A.G., Dejugnat, C., Braun, D., Susha, A., Rogach, A.L., Parak, W.J., Mohwald, H., and Sukhorukov, G.B. 2005 *Nano Lett.* 5, 1371-1377.
- Weissleder, R. 2001 *Nature Biotech.* 19, 316-317.
- West, J.L. and Halas, N.J. 2000 *Current Opinion in Biotech.* 11, 215-217.
- Zharov, V.P., Letfullin, R.R. Galitovskaya, E.N. 2005a *J. Phys. D: Appl. Phys.* 38, 2571-2581.
- Zharov, V.P., Galitovskaya, E.N., Johnson, C., Kelly, T. 2005b *Lasers Surg. Med.* 37, 219-226.
- Zharov, V.P., Mercer, K.E., Galitovskaya, E.N., Smeltzer, M.S. 2006 *Biophys. J.* 90, 619-672.